# 220 GHz E-Plane Transition from Waveguide to Suspended Stripline Integrated on Industrial Organic Laminate Substrate Technology

Victor Fiorese, F. Laporte, J.F. Caillet, G. Catalano, F. Gianesello, Guillaume Ducournau, Emmanuel Dubois, Christophe Gaquière, B. Tricoteaux, M. Werquin, et al.

▶ **To cite this version:**

Victor Fiorese, F. Laporte, J.F. Caillet, G. Catalano, F. Gianesello, et al.. 220 GHz E-Plane Transition from Waveguide to Suspended Stripline Integrated on Industrial Organic Laminate Substrate Technology. European Microwave Conference, EuMC 2021, Session EuMC06 - 3D to 2D Transitions and New Materials for mmWave system Integration, EuMIC/EuMC/EuMW, Apr 2021, London, United Kingdom. pp.99-102, 10.23919/EuMC50147.2022.9784166 . hal-03637651

**HAL Id: hal-03637651**
**https://hal.science/hal-03637651v1**

Submitted on 16 Jun 2022

**HAL** is a multi-disciplinary open access archive for the deposit and dissemination of scientific research documents, whether they are published or not. The documents may come from teaching and research institutions in France or abroad, or from public or private research centers.

L'archive ouverte pluridisciplinaire **HAL**, est destinée au dépôt et à la diffusion de documents scientifiques de niveau recherche, publiés ou non, émanant des établissements d'enseignement et de recherche français ou étrangers, des laboratoires publics ou privés.

# 220 GHz E-Plane Transition from Waveguide to Suspended Stripline Integrated on Industrial Organic Laminate Substrate Technology

V. Fiorese[1,2], F. Laporte[3], J-F. Caillet[3], D. Campos[3], G. Catalano[5], F. Gianesello[1], G. Ducournau[2], E. Dubois[2], C. Gaquière[2,4], B. Tricoteaux[4], M. Werquin[4] & D. Gloria[1]

[1]STMicroelectronics, Crolles, France

[2]IEMN – Institut d'Electronique de Microélectronique et de Nanotechnologie, France

[3]STMicroelectronics, Grenoble, France

[4]MC2-Technologies, France

[5]STMicroelectronics, Italy

victor.fiorese1@st.com

***Abstract*—In this paper, an assessment up to 220 GHz of industrial organic laminate substrate technology to integrate millimeter-wave (mmW) waveguide to suspended stripline (SSL) transition is proposed. A WR5 waveguide transition has been manufactured and insertion loss (IL) of 1.4 dB @ 140 GHz and 4.2 dB @ 220 GHz has been achieved, competing with standard approach using a quartz substrate solution with III-V technology. This promising performance paves the way of cost effective mmW and sub-THz module manufacturing leveraging high volume manufacturing packaging processes developed for Si based technologies.**

***Keywords*—mmW, THz, E-plane transition, low-cost packaging, waveguide, organic laminate substrate.**

## I. Introduction

5G technology being under deployment, preliminary R&D investigations have started to define next cellular technology able to address the never-ending demand of consumer for more mobile data. Spectrum beyond 100 GHz is today foreseen as a promising one to enable 6G technology [1, 2], 252-320 GHz frequency band is a good example with the preliminary IEEE802.15.3d standard being already promoted [3].

Historically, III-V have been the technologies of choice to address mmW applications, but the performance of advanced silicon technologies now enables applications in the mmW and THz spectra from 0.1 to 1THz [4] paving the way for cost-effective solution required by mass market applications. Wireless ICs beyond 100 GHz have already been demonstrated in CMOS [5] and BiCMOS [6] achieving promising performance. However, the deployment of silicon based mmW system operating beyond 100 GHz in the consumer market will also require the development of innovative and cost-effective packaging technology.

So far, the packaging of mmW and THz circuits is achieved using metal waveguide-based assembly [7]. These modules are composed of a thin quartz substrate (~50 µm) on which the IC is assembled and a mechanical package integrating the waveguide components. These packages are machined into metal using computer numerically controlled (CNC) milling. Although excellent performance can be achieved with such an approach, its cost structure and complexity are not compatible with the consumer market.

To overcome this challenge, various innovative techniques have been reported in the literature. Micromachined waveguide packaging techniques, particularly those based on deep reactive silicon etching (DRIE), have been the first one to emerge as a promising solution for developing a low loss and cost-effective packaging solution [8]. Recently, 3D printing technologies have also been considered to complement micromachined waveguide packaging techniques and promising results have been reported up to 330 GHz [9]. Unlike micromachining, 3D printing is an additive manufacturing technique, which means that 3D printed devices are built up layer by layer following a tool-less process. This entails shorter manufacturing time and cost savings due to both the absence of tooling costs and reduced waste.

Dielectric 3D-printing has been considered first and impressive results have been reported in H-band (220-325 GHz), competing with their conventional commercial counterparts [10]. While being lightweight, metal coated dielectric 3D printed device has limited physical rigidity and may require complex process (e.g. for coating complex shapes). Consequently, metallic 3D-printed devices have emerged as an appealing solution for the development of waveguide-based components. The selective laser melting (SLM) metallic 3D printing technology (using < 20µm particle size) has then been evaluated up to the H-band [11]. The surface roughness of SLM technology being a limiting factor, post treatments like manual polishing, gold-electroplating and micromachining [12] have been applied, enabling H-band horn antenna performance to compete with traditional CNC machined parts. However, achievable surface roughness (~ 6 µm) has limited the performances of printed waveguides using SLM [13]. To

improve achievable performance up to H-band, the micro laser sintering (MLS) technology, which uses powder with particle sizes < 5 µm, has been recently proposed [14] to manufacture 3D printed waveguide parts with improved surface roughness without any post processing and consequently reduced loss.

However, while promising solutions have been reported to propose cost effective waveguide-based assembly at mmW, no works has been performed so far on the evaluation of cost-effective substrate technology > 100 GHz. This is the challenge this work tries to address. The paper is organized as following: in section II, we review the E-plane transition design between a WR5 waveguide and a SSL transition fabricated with an organic laminate technology. In section III, the design, assembly and split-block prototypes produced are presented and the measured performances are benchmarked with simulated ones. Finally, section IV provides some conclusion and perspectives.

## II. Design of WR5 E-Plane Transition from Waveguide to SSL on Organic Laminate

In order to assess the quality of WR5 waveguide to E-plane transition, the design of a back-to-back prototype achieved on 2 metallic layers laminated organic substrate has been proposed using HFSS simulations. Key parameters directly linked to IL, such as the amount of dielectric in the waveguide, the backshort length and the probe position have been optimised.

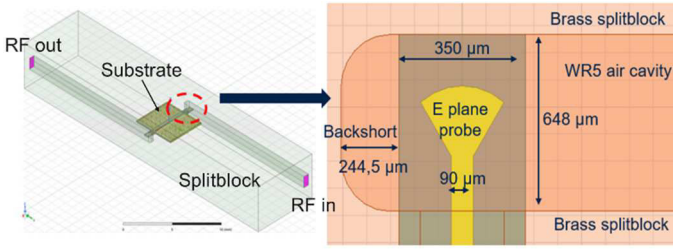


Fig. 1. Substrate in back-to-back simulation bench and top view design

In order to guarantee a uniform ground contact between the substrate ground planes and metallic split-block, a spring contact wire has been applied by wire-bonding at the substrate edges. Gold plating of the split-blocks and laser marking was performed to facilitate wire-bonding. The stack used for substrate is detailed in Figure 2, showing a choice of low-cost, well process-controlled materials to ensure compatibility with a high-volume production perspective.

## III. Split-block Design, Assembly and Measurements

### A. Split-block Assembly Design and Prototyping

The split-block modules were designed to reduce the cost and repeatability of substrate assemblies. The choice of a straight waveguide geometry was defined to minimize as much as possible the number of split-block parts. Alignment pins have been fitted to ensure a constant quality of assembly, as shown in figure 3 representing the CAD model. Two brass split-block modules were micromachined and post-process chemical gilding was performed to avoid oxidation of internal waveguide faces and improve surface quality:

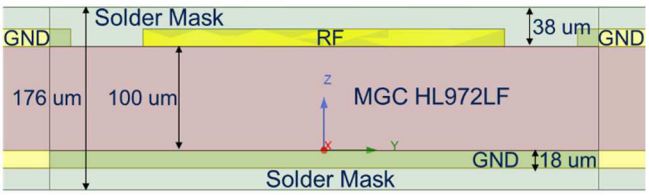


Fig. 2. Substrate stack description

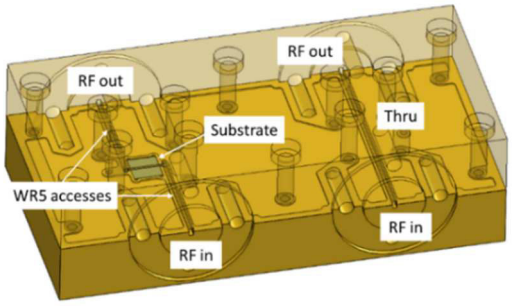


Fig. 3. CAD design of split-block

Split-block design includes a thru structure used to de-embed waveguide accesses contributions. To ensure a homogeneous tightening of both parts of the package, 14 screws have been used. The output connections to external waveguides are ensured by WR5 flanges as shown in Figure 4 :

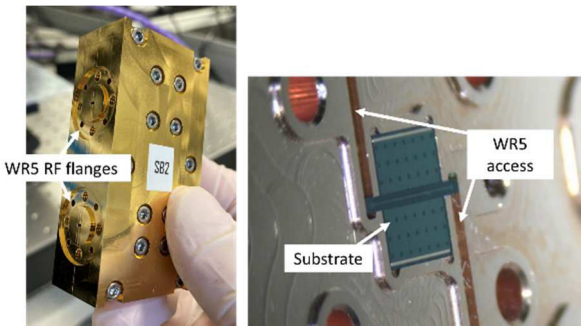


Fig. 4. Micromachined split-block and substrate packaged view

### B. Back-to-Back WR5 E-Plane Measurements

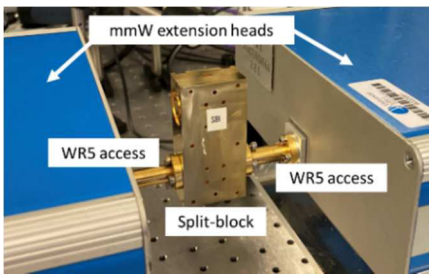


Fig. 5. Manufactured split-block in back-to-back S-parameters measurement setup

In order to include this work in an industrial approach, a design of experiment (DOE) has been proposed to assess the quality of substrate alignment during assembly and the impact

of substrate laser cutting quality on IL. Three several laser sources listed Table 1 have been used to singulate substrates.

Table 1. List of laser processes and suppliers implied during substrate singulations.

| Laser process | Manufacturer | Method |
|---|---|---|
| Femtosecond | IEMN | A |
| Picosecond | ST Agrate | B |
| Nanosecond | EO Technics | C |

Two singulated substrates comprising the E-plane probe and the SSL are shown in Figure 6 below:

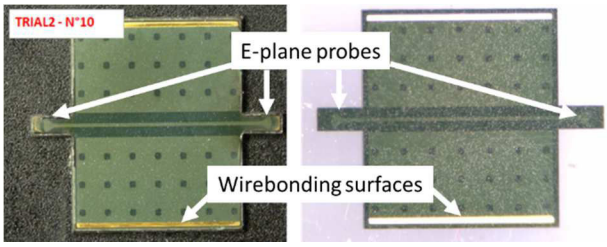


Fig. 6. Substrates in back-to-back configuration singulated with method B (left) and A (right)

Figure 6 also depicts the results of substrate cutting performed with two different laser sources, showing a variation on laser singulation quality. A DOE on E-plane probe positioning was performed, highlighting the impact of the assembly quality on measured IL. Figure 7 below lists the configurations used for DOE on offset and shift values using method A as referenced in Table 1:

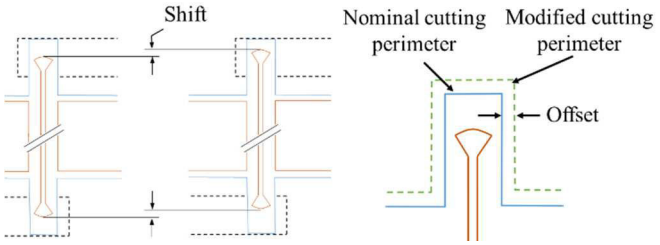


Fig. 7. Illustration of i) a shift in the assembly intentionally introduced and ii) the cutting offset that determines the assembly clearance.

These configurations were obtained by changing the nominal cutting perimeter as shown in Figure 7. The modified cutting was performed with a femtosecond laser with a 7.5 µm laser beam diameter. Figure 8 shows the IL of nominal singulated pieces of substrate, the extreme values of shift and offset of the DOE and the initial simulation performed using Ansys HFSS. Method B demonstrated degraded performance that can be easily explained by the laser cutting quality which obviously degrades the IL due to the heat affected zone (HAZ) [15]. In contrast, a satisfying agreement can be observed between simulation and measurement of other nominal samples following methods A and C. Figure 9 shows the progressive impact of shift values on IL (dB) and an acceptable agreement between simulation and measurement.

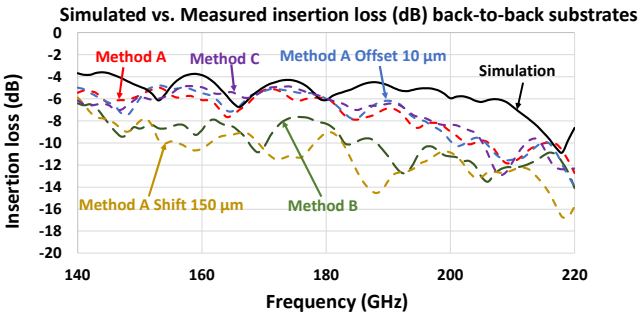


Fig. 8. Simulated back-to-back IL and measurements for methods A, B, C laser singulations and extreme values of DOE parameters.

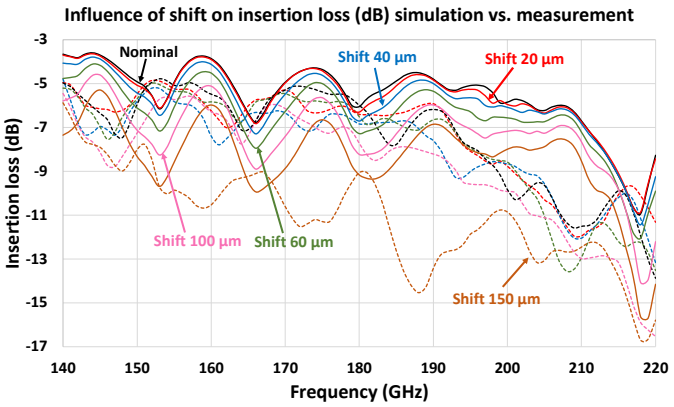


Fig. 9. Simulated (solid lines) and measured (dot lines) IL(dB) with shift variation of substrate in back-to-back

Waveguides contributions to losses were de-embedded thanks to the thru structure measurement. The waveguide length is 17.5 mm for each access and SSL length is 5.74 mm. To de-embed losses in SSL substrate, IL of a SSL were simulated as shown in Figure 10.

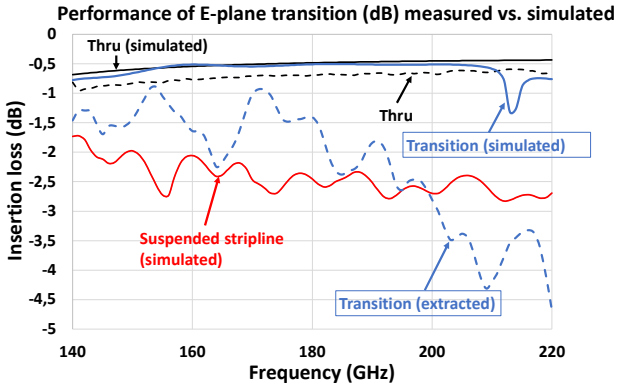


Fig. 10. Simulated and measured IL of E-plane transition and de-embedding structures

IL extracted from measurements for a single transition is 2.5 dB on average between 140-220 GHz, competing with performance obtained with quartz substrate [16].

To complete characterization data, return losses have been simulated and measured for several configurations of shift and offset. Although several definitions exist [17], [18], the hereby used is :

$$RL = 20 \log_{10} |\Gamma| \, . \qquad (1)$$

Where Γ is the reflection coefficient at one of the 2-ports characterized system. An assessment of shift values on this key feature has been performed. Both simulations and measurements at port 1 are described in Figure 11 below :

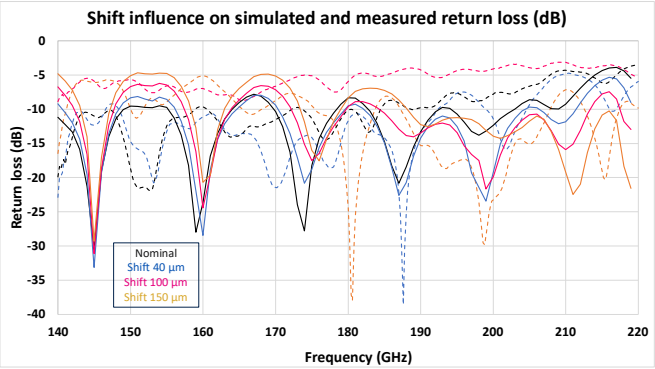


Fig. 11. Shift influence on simulated and measured return losses of one E-plane transition. Simulations and measurements are in solid and dashed lines respectively.

An acceptable agreement is demonstrated between simulated and measured RL values, regardless on chosen shift. The design performances decrease significantly for shift values exceeding 40 µm, which is a reachable tolerance for laser cutting solutions.

## IV. Conclusion & Perspectives

This paper assessed the performance of low-cost packaging leveraging a technology based on an industrial organic laminated substrate characterized in a micromachined split blocks. Measurements in back-to-back configurations highlighted promising performances in terms of insertion loss of 2.5 dB around 200 GHz for a transition between a WR5 guide and a SSL, drawing perspectives for low cost mmW silicon packaging.

## References


[1] T.S. Rappaport., and al., "Wireless Communications and Applications Above 100 GHz: Opportunities and Challenges for 6G and Beyond", IEEE Access, Volume: 7, 2019.

[2] Z Zhang et al. "6G Wireless Networks: Vision, Requirements, Architecture, and Key Technologies", IEEE Vehicular Technology Magazine, Volume 14, Issue 3, 2019.

[3] IEEE802.15 documents. Task Group 3d 100 Gbit/s Wireless (TG3d (100G)). http://www.ieee802.org/15/pub/index_TG3d.html

[4] P. Chevalier et al., "SiGe BiCMOS Current Status and Future Trends in Europe," 2018 IEEE BiCMOS Compd. Semicond. Integr. Circuits Technol. Symp. BCICTS 2018, pp. 64–71, 2018.

[5] I. Abdo et al. "A 300GHz Wireless Transceiver in 65nm CMOS for IEEE802.15.3d Using Push-Push Subharmonic Mixer", IEEE/MTT-S International Microwave Symposium (IMS). 2020.

[6] N. Dolatsha et al., "17.8 A compact 130GHz fully packaged point-to-point wireless system with 3D-printed 26dBi lens antenna achieving 12.5Gb/s at 1.55pJ/b/m", IEEE International Solid-State Circuits Conference (ISSCC), 2017.

[7] J. Treuttel et al., "A 520–620-GHz Schottky Receiver Front-End for Planetary Science and Remote Sensing With 1070 K–1500 K DSB Noise Temperature at Room Temperature", IEEE Transactions On Terahertz Science And Technology, Vol. 6, No. 1, January 2016.

[8] M. Alonso-del Pino et al., "Micromachining for Advanced Terahertz: Interconnects and Packaging Techniques at Terahertz Frequencies", IEEE Microwave Magazine, Volume: 21, Issue: 1, Year: 2020.

[9] B. Zhang et al., "Investigation on 3-D-Printing Technologies for Millimeter- Wave and Terahertz Applications ", Proceedings of the IEEE, Volume: 105, Issue: 4, Year: 2017

[10] A. von Bieren et al., "Monolithic metal-coated plastic components for mm-Wave applications," in Proc. 39th Int. Conf. Infr. Millim. Terahertz Waves, Tucson, TX, USA, Sep. 2014, pp. 1–2..

[11] B. Zhang et al., "Metallic 3D printed antennas for millimeter- and submillimeterwave applications," IEEE Trans. THz Sci. Technol., vol. 6, no. 4, pp. 592–600, Jul. 2016.

[12] Micro Machined Process. BINC, accessed on Dec. 15, 2015. [Online]. Available: http://www.binc.biz/gb/index.php

[13] B. Zhang and H. Zirath, "Metallic 3-D printed rectangular waveguides for millimeter-wave applications," IEEE Comp. Packag. Manuf. Technol., vol. 6, no. 5, pp. 796–804, May 2016.

[14] V. Fiorese et al., "Evaluation of Micro Laser Sintering Metal 3D-Printing Technology for the Development of Waveguide Passive Devices up to 325 GHz", IEEE/MTT-S International Microwave Symposium (IMS), 2020.

[15] R. Le Harzic et al., "Comparison of heat-affected zones due to nanosecond and femtosecond laser pulses using transmission electronic microscopt », Appl. Phys. Lett., vol. 80, no. 21, pp 3886-3888, May 2002.

[16] C. Wang *et al.*, "A Wideband Contactless CPW to W -Band Waveguide Transition," IEEE MIicrowave Wirel. components Lett., vol. 29, no. 11, pp. 2019–2022, 2019.

[17] T. S. Bird, "Definition and misuse of return loss," *IEEE Antennas Propag. Mag.*, vol. 51, no. 2, pp. 166–167, 2009, doi: 10.1109/MAP.2009.5162049.

[18] B. E. Fischer, V. Way, A. Arbor, I. J. Lahaie, V. Way, and A. Arbor, "On the Definition of Return Loss," vol. 55, no. 2, pp. 172–174, 2013.